Available online at www.sciencedirect.com
ScienceDirect
Signal Processing 88 (2008) 1191–1202
SIGNAL PROCESSING
www.elsevier.com/locate/sigpro

A low-complexity adaptive antenna array code acquisition

Hua-Lung Yang, Wen-Rong Wu*

Department of Communication Engineering, National Chiao Tung University, 1001 Ta Hsueh Road, Hsinchu 300, Taiwan , ROC

Received 14 November 2006; received in revised form 21 August 2007; accepted 16 November 2007
Available online 28 November 2007

Abstract

Conventionally, code acquisition with antenna array employs a correlator bank and the serial-search technique. Due to the inherent properties of correlators and serial search, mean acquisition time of the correlator-based approach is large, especially in strong interference environments. Recently, an adaptive-filtering approach has been applied to code acquisition. This method simultaneously performs beamforming and code-delay estimation with a spatial and a temporal filter. Its performance is significantly better than that of the correlator-based approach. However, its computational complexity will be high when the code-delay uncertainty is large. In this paper, we propose a low-complexity adaptive-filtering scheme to solve the problem. Incorporating a serial-search technique, we are able to significantly reduce the size of the temporal filter, so does the computational complexity. We also analyze the proposed algorithm and derive closed-form expressions for optimum solutions, mean-squared error, and mean acquisition time. Simulations show that while the proposed system somewhat compromises the performance, the computational complexity is much lower that of the original adaptive-filtering approach.

Keywords: Code acquisition; Adaptive filter; Antenna array; DS/CDMA

1. Introduction

Direct-sequence/code-division multiple access (DS/CDMA) is a promising technique for wireless mobile communication. It is well known that the main performance bottleneck for a CDMA system is multiple access interference (MAI). MAI not only affects data detection, but also code acquisition. Code acquisition is the first operation that a CDMA receiver has to perform. It attempts to align the local code sequence and the received desired signal with a difference less than a chip duration. After successful code acquisition, other operations such as channel estimate, code tracking, and data detection can follow. Thus, code acquisition is a critical task in DS/CDMA systems.

Code acquisition for single antenna systems has been extensively studied in the literature [1–11] (and reference therein). The correlator approach [1–4] is most well known. However, the correlator is only optimal for the single-user case. Its performance degrades significantly when MAI presents [4]. Subspace- and matrix-based methods [5,6] have been developed to solve the problem. The advantage of subspace-based approaches is that no training sequences are required and the performance is much better than that of the correlator approach. However, these methods usually have to estimate,

*Corresponding author. Tel.: +886 3 5712121x54529.
E-mail addresses: hualungyang.cm90g@nctu.edu.tw (H.-L. Yang), wrwu@faculty.nctu.edu.tw (W.-R. Wu).

0165-1684/$ - see front matter © 2007 Elsevier B.V. All rights reserved.
doi:10.1016/j.sigpro.2007.11.008

decompose, or inverse the autocorrelation matrix. This often requires high computational complexity, especially for systems with large processing gains. Recently, adaptive-filtering technique has been introduced to code acquisition [7–11]. It is claimed that [7], the adaptive-filtering approach can provide higher acquisition-based capacity [3] compared to the correlator methods. The acquisition-based capacity indicates the maximal number of users that a system can tolerate with a given acquisition error rate. One problem with the adaptive-filtering scheme [7] is that its computational complexity grows linearly along with the code-delay uncertainty range. A low-complexity scheme was then developed in [11].

It is well known that antenna arrays can significantly enhance acquisition performance [12–14]. In [12], each array element is equipped with a correlator, and the correlator outputs serve the inputs of a beamformer. When directional MAI presents, matrix inversion is required to derive the beamformer weights [12]. In [13], an adaptive beamformer is used to avoid the problem. However, in the presence of directional MAI, it requires a long adaptation period and the acquisition is slow. To solve the problem, an adaptive-filter-based array system was then proposed [15,16]. This system simultaneously performs adaptive beamforming and code-delay estimation with a spatial and a temporal filter. The code delay can then be estimated with the peak position of the temporal filter. It has been shown that the approach significantly outperforms the correlator-based system in [13].

Similar to the conventional adaptive-filtering acquisition, the computational complexity of the temporal filter in [15] grows linearly along with the uncertain range of the code delay. When the range is large, the computational complexity may be high. In this paper, we propose a low-complexity adaptive array code acquisition scheme to solve the problem. The main idea is to divide the whole delay uncertainty range into several (delay) cells, and then sequentially search for the code delay of the desired user among those cells. This is essentially a serial-search-technique, being able to shorten the filter length of the temporal filter. As a result, the computational complexity can be reduced. As that in [15], the proposed system employs a criterion such that both filters can be simultaneously adjusted by a constrained least-mean-square (LMS) algorithm. However, the acquisition process is more involved than that in [15]. This is because one additional decision has to be made before the code delay can be estimated. For each tested cell, filters are first adapted for a period time to determine if the code delay falls into the cell's delay region or not. If it does, the spatial filter will act as a minimum mean-squared error (MMSE) beamformer and the temporal filter as a code-delay estimator. Thus, the code delay can then be estimated with the peak position of the temporal filter. If not, the next cell is tested and the process is repeated. Note that if the code delay does not fall into the tested cell's region, the spatial filter will act as a signal blocker with its weighs all being zeros. This property is then used to derive an index for the cell testing. With the choice of the number of cells, we can have an easy tradeoff between performance and complexity. In many cases, however, the complexity reduction is large, but the performance loss is still acceptable. In this paper, we only consider flat-fading channels for simplicity. It is straightforward to extend the proposed algorithm to multipath environments. Also note that with the proposed architecture, we can also apply other types of adaptive algorithms such as the recursive least-squares (RLS) algorithm. In this case, the overall performance can be greatly enhanced, but the computational complexity is also significantly increased.

This paper is organized as follows. Section 2 develops the proposed algorithm. Section 3 discusses issues of adaptive implementation, and Section 4 carries out performance analysis. Section 5 presents simulation results demonstrating the effectiveness of the proposed scheme. Finally, Section 6 draws conclusions. Throughout this paper, we use $\mathbf{I}$, $\|\cdot\|$, and $E\{\cdot\}$ to denote an identity matrix, a vector two-norm, and a statistical expectation operator, respectively. Also, let $\mathrm{i}=\sqrt{-1}$ and $(\cdot)^*$, $(\cdot)^{\mathrm{T}}$, and $(\cdot)^{\mathrm{H}}$ denote the complex conjugate, transpose, and Hermitian operator, respectively.

2. Proposed low-complexity code acquisition

Consider that there are K users in a mobile cell and each user is given an aperiodic pseudo-noise (PN) code sequence with a period much longer than a symbol period. The transmitted signal of the kth user in baseband can be expressed as

$$x_k(t)=\sum_{j=-\infty}^{\infty} d_k(j)\sum_{l=0}^{U-1} c_{k,j}(l)p(t-lT_{\mathrm{c}}-jUT_{\mathrm{c}}), \qquad (1)$$

$k = 1, \ldots, K$, where $d_k(j)$ is the jth BPSK symbol of the kth user, $c_{k,j}(l)$ the lth chip of the spreading signal for $d_k(j)$, $p(t)$ a unit-amplitude rectangular chip-pulse with a chip-duration T_c, and U the number of chips in a symbol. At the receiver, a uniformly linear array with M sensors is placed and the element spacing is assumed to be half a wavelength of the carrier. Then, the chip-rate sampled received signal vector in baseband can be represented as

$$\mathbf{r}(n) = \sum_{k=1}^{K} \mathbf{a}_k \alpha_k x_k(n - \tau_k) \exp(-\mathrm{i}\theta_k) + \boldsymbol{\eta}(n), \tag{2}$$

where code delays τ_k, $k = 1, \ldots, K$ are assumed to be integers between $[0, U)$, and $\boldsymbol{\eta}(n)$ is an $M \times 1$, complex, and zero-mean Gaussian noise vector with a covariance matrix $\sigma_\eta^2 \mathbf{I}$. Also, $\mathbf{a}_k$, α_k, and θ_k stand for the steering vector, the amplitude, and the carrier-phase offset, associated with the kth user, respectively. Note that θ_k is uniformly distributed over $[-\pi, \pi)$ and $\mathbf{a}_k$ is given by $\mathbf{a}_k = [1, \exp(-\mathrm{i}\pi \sin \phi_k), \ldots, \exp(-\mathrm{i}\pi(M-1) \sin \phi_k)]^{\mathrm{T}}$, where ϕ_k denotes the direction-of-arrival (DoA) of the kth user's signal. Without loss of generality, the first user is seen as the desired user. We also assume that $d_1(j) = 1$ during the acquisition period.

As described, the whole delay uncertainty U is divided into cells. Let $Q = \lceil U/M_t \rceil$, where M_t denotes the filter length of the temporal filter. Among these Q cells, the actual code delay only falls into the delay region of a certain cell. Let the cell whose delay region includes the desired code delay be the inphase cell and others be outphase cells. Thus, we have one inphase cell and $Q-1$ outphase cells.

Fig. 1 illustrates the block diagram of the proposed system. As seen, the spatial filter $\mathbf{w}_s^q$ combines M array outputs into a single output, where $q = 0, \ldots, Q-1$ denotes the cell index. The temporal filter $\mathbf{w}_t^q$ uses $x_1(n - qM_t)$ as its input signal and the spatial filter output as its reference signal, where $x_1(n)$ is the desired user's PN sequence [since $d_1(j) = 1$]. As far as an inphase cell is concerned, the system is the same as that in [16]. From Fig. 1, we can see that the spatial filter can act like a beamformer to reject interference, while the temporal filter can be a code-delay estimator. In other words, the optimum temporal filter will have a unique peak weight whose location corresponds to the code delay [16]. However, for the outphase cells,

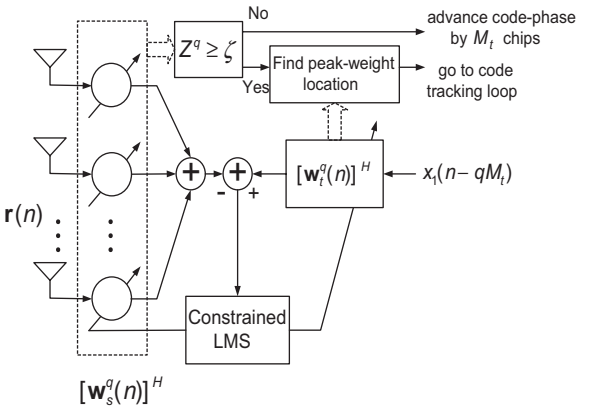

Fig. 1. System diagram of the proposed system, where $Z^q = \|\mathbf{w}_s^q(N)\|^2$, $q = 0, \ldots, Q-1$.

there is no correlation between the input and the reference signals. The optimum spatial filter will become a signal blocker (all weights are zeros). Using the characteristic, we propose to perform cell detection with the magnitude of the spatial filter weights. If $\|\mathbf{w}_s^{q'}\|^2$ exceeds a preset threshold, then the q'th cell is considered as the inphase cell. Once the inphase cell is identified, the peak weight in $\mathbf{w}_t^{q'}$ can be located. Let the peak weight be $w_{t,\hat{\Delta}}^{q'}$, where $w_{t,\hat{\Delta}}^{q'}$ with $0 \leqslant \hat{\Delta} < M_t$ denotes the $(\hat{\Delta}+1)$th element of $\mathbf{w}_t^{q'}$. Then, the code delay can be estimated with $\hat{\tau}_1 = q' M_t + \hat{\Delta}$.

As shown, the difference between these two-filter outputs forms the error signal from which we can perform minimization. The cost function to minimize is the same as that in [16]. For each cell, we let

$$\bar{J}^q = E\{|[\mathbf{w}_t^q]^{\mathrm{H}} \mathbf{x}^q(n) - [\mathbf{w}_s^q]^{\mathrm{H}} \mathbf{r}(n)|^2\}, \tag{3}$$

$q = 0, \ldots, Q-1$, where $\mathbf{w}_s^q \triangleq [w_{s,0}^q, \ldots, w_{s,M-1}^q]^{\mathrm{T}}$, $\mathbf{w}_t^q \triangleq [w_{t,0}^q, \ldots, w_{t,M_t-1}^q]^{\mathrm{T}}$, and $\mathbf{x}^q(n) \triangleq [x_1(n - qM_t), x_1(n - qM_t - 1), \ldots, x_1(n - qM_t - M_t + 1)]^{\mathrm{T}}$. From (3), it is simple to observe that a minimum $\bar{J}^q$ (which is zero) occurs at $\mathbf{w}_t^q = \mathbf{0}$ and $\mathbf{w}_s^q = \mathbf{0}$, and this is an undesired trivial solution. To avoid that, we have to make a constraint on the solution. Here, we pose a unit-norm constraint, i.e.,

$$\|\mathbf{w}_t^q\|^2 \triangleq [\mathbf{w}_t^q]^{\mathrm{H}} \mathbf{w}_t^q = 1, \quad q = 0, \ldots, Q-1. \tag{4}$$

Thus, minimization of (3) turns out to be a constrained optimization problem. We use the Lagrange multiplier method [17] to transform the constrained optimization problem into an unconstrained one. From (3) and (4), we have an

equivalent cost function as

$$J^q = E\{|[\mathbf{w}_t^q]^H\mathbf{x}^q(n) - [\mathbf{w}_s^q]^H\mathbf{r}(n)|^2\} + \xi^q\{1 - [\mathbf{w}_t^q]^H\mathbf{w}_t^q\}$$
$$= [\mathbf{w}_t^q]^H\mathbf{R}_x^q\mathbf{w}_t^q + [\mathbf{w}_t^q]^H\mathbf{K}^q\mathbf{w}_s^q + [\mathbf{w}_s^q]^H[\mathbf{K}^q]^H\mathbf{w}_t^q + [\mathbf{w}_s^q]^H\mathbf{R}_r\mathbf{w}_s^q + \xi^q\{1 - [\mathbf{w}_t^q]^H\mathbf{w}_t^q\}, \quad (5)$$

where

$$\mathbf{K}^q_{(M_t\times M)} \triangleq -E\{\mathbf{x}^q(n)\mathbf{r}^H(n)\}, \quad (6)$$

$$\mathbf{R}_{r(M\times M)} \triangleq E\{\mathbf{r}(n)\mathbf{r}^H(n)\},$$
$$\mathbf{R}^q_{x(M_t\times M_t)} \triangleq E\{\mathbf{x}^q(n)[\mathbf{x}^q(n)]^H\},$$

and ξ^q denotes the Lagrange multiplier for the qth cell. Differentiating (5) with respect to $[\mathbf{w}_s^q]^*$ and $[\mathbf{w}_t^q]^*$ and setting the results to be zero-vectors, we obtain

$$\frac{\partial J^q}{\partial[\mathbf{w}_s^q]^*} = [\mathbf{K}^q]^H\mathbf{w}_t^q + \mathbf{R}_r\mathbf{w}_s^q = \mathbf{0}, \quad (7)$$

$$\frac{\partial J^q}{\partial[\mathbf{w}_t^q]^*} = \mathbf{R}_x^q\mathbf{w}_t^q + \mathbf{K}^q\mathbf{w}_s^q - \xi^q\mathbf{w}_t^q = \mathbf{0}. \quad (8)$$

Since $\mathbf{R}_r$ is a full rank matrix, its matrix inversion exists. From (7), we have

$$\mathbf{w}_s^q = -\mathbf{R}_r^{-1}[\mathbf{K}^q]^H\mathbf{w}_t^q. \quad (9)$$

Substituting (9) into (8), we have

$$\{\mathbf{R}_x^q - \mathbf{K}^q\mathbf{R}_r^{-1}[\mathbf{K}^q]^H\}\mathbf{w}_t^q - \xi^q\mathbf{w}_t^q = \mathbf{0}. \quad (10)$$

It is simple to observe that the solution of ξ^q in (10) denotes the eigenvalue of $\mathbf{R}_x^q - \mathbf{K}^q\mathbf{R}_r^{-1}[\mathbf{K}^q]^H$, while $\mathbf{w}_t^q$ is the corresponding eigenvector. Note that an eigenvector $\mathbf{w}_t^q$ satisfies (4) automatically. Once $\mathbf{w}_t^q$ is derived, $\mathbf{w}_s^q$ can be found using (9). Multiplying (10) with $[\mathbf{w}_t^q]^H$, we obtain

$$\xi^q = [\mathbf{w}_t^q]^H\{\mathbf{R}_x^q - \mathbf{K}^q\mathbf{R}_r^{-1}[\mathbf{K}^q]^H\}\mathbf{w}_t^q. \quad (11)$$

Substituting (9) into (5) and using (11), we have

$$J^q = [\mathbf{w}_t^q]^H\mathbf{R}_x^q\mathbf{w}_t^q - [\mathbf{w}_t^q]^H\{\mathbf{K}^q\mathbf{R}_r^{-1}[\mathbf{K}^q]^H\}\mathbf{w}_t^q - [\mathbf{w}_t^q]^H\{\mathbf{K}^q\mathbf{R}_r^{-1}[\mathbf{K}^q]^H\}\mathbf{w}_t^q + [\mathbf{w}_t^q]^H\{\mathbf{K}^q\mathbf{R}_r^{-1}[\mathbf{K}^q]^H\}\mathbf{w}_t^q$$
$$= [\mathbf{w}_t^q]^H\{\mathbf{R}_x^q - \mathbf{K}^q\mathbf{R}_r^{-1}[\mathbf{K}^q]^H\}\mathbf{w}_t^q = \xi^q, \quad (12)$$

which is identical to (11) exactly. Let solutions to (7)–(8), which are optimum weights, be $\mathbf{w}^q_{s,o}$ and $\mathbf{w}^q_{t,o}$, and the corresponding minimum value of (12) be $J^q_{\min}$. We then conclude that $J^q_{\min}$ is equal to the minimum eigenvalue $\mathbf{R}_x^q - \mathbf{K}^q\mathbf{R}_r^{-1}[\mathbf{K}^q]^H$ and $\mathbf{w}^q_{t,o}$ is the corresponding eigenvector. Substituting $\mathbf{w}^q_{t,o}$ into (9), we can then obtain $\mathbf{w}^q_{s,o}$.

To simplify notations, we rewrite (2) as

$$\mathbf{r}(n) = \sum_{k=1}^{K}\mathbf{a}_k\alpha_k x_k(n-\tau_k)\exp(-i\theta_k) + \boldsymbol{\eta}(n) \quad (13)$$
$$= \mathbf{a}\exp(-i\theta)x(n - vM_t - \Delta) + \sum_{k=2}^{K}\mathbf{a}_k\alpha_k x_k(n-\tau_k)\exp(-i\theta_k) + \boldsymbol{\eta}(n), \quad (14)$$

where we let $\mathbf{a}_1 = \mathbf{a}$, $\alpha_1 = 1$, $\theta_1 = \theta$, $x_1(n) = x(n)$, and $\tau_1 = vM_t + \Delta$. It is simple to see that the inphase cell is the cell that $q = v$.

We first consider the scenario of the inphase cell. As mentioned, the proposed system is just the same as that in [16]. From [16], we can have

$$\xi^v_{\min} = J^v_{\min} = 1 - \mathbf{a}^H\mathbf{R}_r^{-1}\mathbf{a}, \quad (15)$$

$$\mathbf{w}^v_{t,o} = [\underbrace{0,\ldots,0}_{\Delta},1,0,\ldots,0]^T\exp(i\psi), \quad (16)$$

$$\mathbf{w}^v_{s,o} = \mathbf{R}_r^{-1}\mathbf{a}\exp(-i[\theta-\psi]), \quad (17)$$

where ψ is an arbitrary angle. From (16) and (17), we can see that both filters do not have unique solutions. This is not surprising since we only pose the magnitude constraint. Also, note that $\mathbf{w}^v_{s,o}$ is just the conventional MMSE beamformer ($\mathbf{R}_r^{-1}\mathbf{a}$).

Now, let us consider the remaining $Q-1$ outphase cells. Since $q \neq v$, we have $\mathbf{K}^q = \mathbf{0}$ [see (6)]. Then, (5) becomes

$$J^q = [\mathbf{w}_s^q]^H\mathbf{R}_r\mathbf{w}_s^q + [\mathbf{w}_t^q]^H\mathbf{R}_x^q\mathbf{w}_t^q + \xi^q\{1 - [\mathbf{w}_t^q]^H\mathbf{w}_t^q\}, \quad (18)$$

$q \neq v$, where $\mathbf{R}_x^q = \mathbf{I}$ (the long-code assumption). Also, (7)–(8) become

$$\frac{\partial J^q}{\partial[\mathbf{w}_s^q]^*} = \mathbf{R}_r\mathbf{w}_s^q = \mathbf{0}, \quad (19)$$

$$\frac{\partial J^q}{\partial[\mathbf{w}_t^q]^*} = \mathbf{w}_t^q - \xi^q\mathbf{w}_t^q = \mathbf{0}. \quad (20)$$

From (19), we have $\mathbf{w}^q_{s,o} = \mathbf{0}$, since $\mathbf{R}_r$ is a full-rank matrix. The spatial filter will block all signal from entering the temporal filter. From (20), we can see $\xi^q_{\min} = J^q_{\min} = 1$, and there is no unique solution for $\mathbf{w}^q_{t,o}$ either. Any vector satisfies the unit-norm constraint can serve as an optimum solution.

3. Adaptive implementation and convergence analysis

In Section 2, we have proposed a low-complexity code acquisition system modifying the system in

[16]. Optimum weights of the filters are derived with the eigen-decomposition technique. However, the required computational complexity of eigen-decomposition is on the order of $\mathcal{O}(M_t^3)$. In addition, the matrix inversion of $\mathbf{R}_r$ is required in (10). To alleviate these problems, we propose to use an adaptive algorithm to derive the optimum filter weights. The adaptive algorithm we consider is the LMS algorithm which is well known for its simplicity and robustness. As shown, we have a unit-norm constraint on the temporal filter. Applying this constraint, we then obtain a constrained LMS algorithm. In what follows, we will describe the algorithm and examine related issues such as the step size bound and steady-state mean-squared error (MSE). Besides, we also analyze the output SINR of beamformer [see $\gamma(n)$ in Fig. 1] for an inphase cell.

3.1. Constrained LMS and convergence issue

Rewriting (3), we have

$$\bar{J}^q(n) = [\mathbf{w}_v^q(n)]^{\mathrm{H}} \mathbf{R}_v^q \mathbf{w}_v^q(n), \quad q = 0, \ldots, Q-1, \tag{21}$$

where

$$\mathbf{w}_v^q(n) \triangleq [[\mathbf{w}_t^q(n)]^{\mathrm{T}}, [\mathbf{w}_s^q(n)]^{\mathrm{T}}]^{\mathrm{T}},$$
$$\mathbf{v}^q(n) \triangleq [[\mathbf{x}^q(n)]^{\mathrm{T}}, -\mathbf{r}^{\mathrm{T}}(n)]^{\mathrm{T}},$$

and

$$\mathbf{R}_v^q \triangleq E\{\mathbf{v}^q(n)[\mathbf{v}^q(n)]^{\mathrm{H}}\}.$$

The gradient of (21) is by

$$\frac{\partial \bar{J}^q(n)}{\partial [\mathbf{w}_v^q(n)]^*} = \mathbf{R}_v^q \mathbf{w}_v^q(n). \tag{22}$$

Using (22), we can apply a gradient decent algorithm to obtain the optimum solution, denoted as $\mathbf{w}_{v,\mathrm{o}}^q$. However, $\mathbf{R}_v^q$ needs to be estimated. The simplest estimate of $\mathbf{R}_v^q$ is to use instantaneous value from $\mathbf{v}^q(n)[\mathbf{v}^q(n)]^{\mathrm{H}}$ and this yields a stochastic gradient decent algorithm, called the LMS algorithm [17]. We then can have the filter adaptation as

$$\mathbf{w}_v^q(n+1) = \mathbf{w}_v^q(n) + \mu\{-\mathbf{v}^q(n)[\mathbf{v}^q(n)]^{\mathrm{H}} \mathbf{w}_v^q(n)\}, \tag{23}$$

where μ is the step size controlling the convergence rate. Recall that we have the constraint $\|\mathbf{w}_t^q(n)\| = 1$. This constraint can be easily satisfied if normalization is performed on $\mathbf{w}_t^q(n)$ at every iteration. The overall adaptation procedure is given as

$$e^q(n) = [\mathbf{w}_v^q(n)]^{\mathrm{H}} \mathbf{v}^q(n), \tag{24}$$

$$\mathbf{H}^q(n) = \mathrm{diag}\left\{ \underbrace{\frac{1}{\|\mathbf{w}_t^q(n)\|}, \ldots, \frac{1}{\|\mathbf{w}_t^q(n)\|}}_{M_t}, \underbrace{1, \ldots, 1}_{M} \right\}, \tag{25}$$

$$\mathbf{w}_v^q(n+1) = \mathbf{H}^q(n)\mathbf{w}_v^q(n) - \mu \mathbf{v}^q(n)[e^q(n)]^*, \tag{26}$$

$n = 0, 1, \ldots, N-1$; $q = 0, \ldots, Q-1$, where $\mathrm{diag}\{\cdot\}$ denotes a diagonal matrix consisting of the arguments that it includes, and N the iteration number for each cell. As we can see, $\mathbf{H}^q(n)$ normalizes $\mathbf{w}_t^q(n)$ at every iteration. After training, we have to detect the inphase cell first. To do that, we propose to compare $\|\mathbf{w}_s^q(N)\|^2$ with a preset threshold. If $\|\mathbf{w}_s^q(N)\|^2$ is larger than the threshold, the cell is deemed as the inphase cell. Then, the peak location of $\mathbf{w}_t^q(N)$ is located and the code delay is estimated. Otherwise, we go to the next cell and start the process all over again. To guarantee convergence, μ has to be selected properly. Here, we perform the mean convergence analysis to derive a step size bound. Subtracting $\mathbf{w}_{v,\mathrm{o}}^q = [[\mathbf{w}_{t,\mathrm{o}}^q]^{\mathrm{T}}, [\mathbf{w}_{s,\mathrm{o}}^q]^{\mathrm{T}}]^{\mathrm{T}}$ from both sides of (26), we have

$$\begin{aligned}
\Delta\mathbf{w}_v^q(n+1) &= \Delta\mathbf{w}_v^q(n) + [\mathbf{H}^q(n) - \mathbf{I}]\mathbf{w}_v^q(n) \\
&\quad - \mu\mathbf{v}^q(n)\{[\mathbf{w}_v^q(n)]^{\mathrm{H}}\mathbf{v}^q(n)\}^* \\
&= \Delta\mathbf{w}_v^q(n) + [\mathbf{H}^q(n) - \mathbf{I}]\mathbf{w}_v^q(n) \\
&\quad - \mu\mathbf{v}^q(n)[\mathbf{v}^q(n)]^{\mathrm{H}}[\Delta\mathbf{w}_v^q(n) + \mathbf{w}_{v,\mathrm{o}}^q] \\
&= \{\mathbf{I} - \mu\mathbf{v}^q(n)[\mathbf{v}^q(n)]^{\mathrm{H}}\}\Delta\mathbf{w}_v^q(n) \\
&\quad + [\mathbf{H}^q(n) - \mathbf{I}]\mathbf{w}_v^q(n) - \mu\mathbf{v}^q(n)[e_{\mathrm{o}}^q(n)]^*,
\end{aligned} \tag{27}$$

where $e_{\mathrm{o}}^q(n) \triangleq [\mathbf{w}_{v,\mathrm{o}}^q]^{\mathrm{H}}\mathbf{v}^q(n)$ and $\Delta\mathbf{w}_v^q(n) \triangleq \mathbf{w}_v^q(n) - \mathbf{w}_{v,\mathrm{o}}^q$. Taking the statistical expectation of (27), applying the direct-averaging method [17], and using the orthogonality principle, we then have

$$\begin{aligned}
E\{\Delta\mathbf{w}_v^q(n+1)\} &= [\mathbf{I} - \mu\mathbf{R}_v^q]E\{\Delta\mathbf{w}_v^q(n)\} \\
&\quad + [E\{\mathbf{H}^q(n)\} - \mathbf{I}]E\{\mathbf{w}_v^q(n)\}.
\end{aligned} \tag{28}$$

Let $\mathbf{\Lambda}^q = \mathrm{diag}\{\lambda_{v,1}^q, \ldots, \lambda_{v,M_t+M}^q\}$ with $\lambda_{v,j}^q$ being an eigenvalue of $\mathbf{R}_v^q$, and $\mathbf{U}^q$ be a matrix consisting of the eigenvectors of $\mathbf{R}_v^q$. Multiplying (28) with $[\mathbf{U}^q]^{\mathrm{H}}$ and letting $\mathbf{g}^q(n) = [\mathbf{U}^q]^{\mathrm{H}}E\{\Delta\mathbf{w}_v^q(n)\}$, we obtain

$$\begin{aligned}
\mathbf{g}^q(n+1) &= [\mathbf{I} - \mu\mathbf{\Lambda}^q]\mathbf{g}^q(n) \\
&\quad + [\mathbf{U}^q]^{\mathrm{H}}[E\{\mathbf{H}^q(n)\} - \mathbf{I}]E\{\mathbf{w}_v^q(n)\}.
\end{aligned} \tag{29}$$

Since $\mathbf{w}_t^q(n)$ is normalized at every iteration and the step size is usually small, it is reasonable to assume that $\mathbf{H}^q(n) \approx \mathbf{I}$ and the second term in the right-hand

side of (29) can be ignored. Iterating (29), we obtain

$$\mathbf{g}^q(n) = [\mathbf{I} - \mu\mathbf{\Lambda}^q]^n \mathbf{g}^q(0). \tag{30}$$

Thus, for (29) to converge, the following condition must be satisfied:

$$0 < \mu < \frac{2}{\lambda^q_{v,\max}}, \tag{31}$$

where $\lambda^q_{v,\max}$ denotes the maximum eigenvalue of $\mathbf{R}^q_v$. This result is the same as that of the conventional LMS algorithm [17]. From (30), we can also see that $\mathbf{g}^q(\infty) = \mathbf{0}$. In other words, $E\{\mathbf{w}^q_v(n)\} = \mathbf{w}^q_{v,\mathrm{o}}$, when $n \to \infty$.

Note that while the conventional LMS algorithm requires $2(M_\mathrm{t} + M)$ multiplications per iteration, the constrained LMS algorithm developed here needs extra M_t multiplications for calculation of $\|\mathbf{w}^q_\mathrm{t}(n)\|$ and extra M_t divisions for normalization [see (26)].

3.2. Steady-state MSE analysis

We now derive the steady-state MSE of the constrained LMS algorithm. Invoking the direct-averaging method [17] and using (27), we can write the correlation matrix of the tap-weight error vector as

$$\begin{aligned}\mathbf{P}^q(n+1) &\triangleq E\{\Delta\mathbf{w}^q_v(n+1)[\Delta\mathbf{w}^q_v(n+1)]^\mathrm{H}\} \\ &= [\mathbf{I} - \mu\mathbf{R}^q_v]\mathbf{P}^q(n)[\mathbf{I} - \mu\mathbf{R}^q_v] + \mu^2 J^q_{\min}\mathbf{R}^q_v \\ &\quad + E\{[\mathbf{H}^q(n) - \mathbf{I}]\mathbf{w}^q_v(n) \\ &\quad \times[\mathbf{w}^q_v(n)]^\mathrm{H}[\mathbf{H}^q(n) - \mathbf{I}]\}. \end{aligned} \tag{32}$$

As stated, $\mathbf{w}^q_\mathrm{t}(n)$ is normalized at every iteration and the step size is usually small. Thus, $\mathbf{H}^q(n) \approx \mathbf{I}$ and the last term in the right-hand side of (32) can be ignored. Let $\bar{\mathbf{P}}^q(n) \triangleq [\mathbf{U}^q]^\mathrm{H}\mathbf{P}^q(n)\mathbf{U}^q$ and observe that $[\mathbf{U}^q]^\mathrm{H}\mathbf{R}^q_v\mathbf{U}^q = \mathbf{\Lambda}^q$. Pre-multiplying and post-multiplying both sides of (32) with $[\mathbf{U}^q]^\mathrm{H}$ and $\mathbf{U}^q$, respectively, we have

$$\bar{\mathbf{P}}^q(n+1) = [\mathbf{I} - \mu\mathbf{\Lambda}^q]\bar{\mathbf{P}}^q(n)[\mathbf{I} - \mu\mathbf{\Lambda}^q] + \mu^2 J^q_{\min}\mathbf{\Lambda}^q. \tag{33}$$

Let the jth element on the diagonal of $\bar{\mathbf{P}}^q(n)$ be $\bar{p}^q_j(n)$. Then,

$$\bar{p}^q_j(n+1) = (1 - \mu\lambda^q_{v,j})^2\bar{p}^q_j(n) + \mu^2 J^q_{\min}\lambda^q_{v,j}, \tag{34}$$

$j = 1, \ldots, M_\mathrm{t} + M$. When $n \to \infty$, $\bar{p}^q_j(n+1) \approx \bar{p}^q_j(n)$. From (34), we derive

$$\bar{p}^q_j(\infty) = \frac{\mu J^q_{\min}}{2 - \mu\lambda^q_{v,j}}. \tag{35}$$

The additional MSE due to the use of the LMS algorithm is generally referred to as the excess MSE, denoted as $J^q_{\mathrm{ex}}(\infty)$. From [17], we then have

$$J^q_{\mathrm{ex}}(\infty) = \sum_{j=1}^{M_\mathrm{t}+M} \bar{p}^q_j(\infty)\lambda^q_{v,j} = J^q_{\min}\sum_{j=1}^{M_\mathrm{t}+M}\frac{\mu\lambda^q_{v,j}}{2 - \mu\lambda^q_{v,j}}. \tag{36}$$

Denote the steady-state MSE of the LMS adaptation as J^q_{ss}. Finally, we have

$$J^q_{\mathrm{ss}} = J^q_{\min} + J^q_{\mathrm{ex}}(\infty). \tag{37}$$

3.3. Output SINR at beamformer for an inphase cell

Now, let us analyze the output SINR of the beamformer. We consider the inphase cell ($q = v$), and the output is by

$$\gamma(n) \triangleq [\mathbf{w}^v_\mathrm{s}(n)]^\mathrm{H}\mathbf{r}(n) \tag{38}$$

$$= [\mathbf{w}^v_\mathrm{s}(n)]^\mathrm{H}(\mathbf{a}\exp(-\mathrm{i}\theta)x(n - vM_\mathrm{t} - \Delta) + \mathbf{z}(n)), \tag{39}$$

where $\mathbf{z}(n)$ consists of MAI and noise. Using (17), we can find the output SINR of the optimum beamformer, denoted as SINR_o, as

$$\mathrm{SINR}_\mathrm{o} = \frac{[\mathbf{w}^v_{\mathrm{s,o}}]^\mathrm{H}\mathbf{R}_A\mathbf{w}^v_{\mathrm{s,o}}}{[\mathbf{w}^v_{\mathrm{s,o}}]^\mathrm{H}\mathbf{R}_z\mathbf{w}^v_{\mathrm{s,o}}} \tag{40}$$

$$= \frac{\mathbf{a}^\mathrm{H}\mathbf{R}_r^{-1}\mathbf{R}_A\mathbf{R}_r^{-1}\mathbf{a}}{\mathbf{a}^\mathrm{H}\mathbf{R}_r^{-1}\mathbf{R}_z\mathbf{R}_r^{-1}\mathbf{a}}, \tag{41}$$

where $\mathbf{R}_A = \mathbf{a}\mathbf{a}^\mathrm{H}$ and $\mathbf{R}_z \triangleq E\{\mathbf{z}(n)\mathbf{z}^\mathrm{H}(n)\}$. Since we use adaptive filter-weights to approximate the optimum weights, we have to include the excess MSE in the SINR calculation. Thus, we can rewrite (41) as

$$\mathrm{SINR}_\mathrm{o} = \frac{\mathbf{a}^\mathrm{H}\mathbf{R}_r^{-1}\mathbf{R}_A\mathbf{R}_r^{-1}\mathbf{a}}{\mathbf{a}^\mathrm{H}\mathbf{R}_r^{-1}\mathbf{R}_z\mathbf{R}_r^{-1}\mathbf{a} + J^v_{\mathrm{ex}}(\infty)}, \tag{42}$$

where $J^v_{\mathrm{ex}}(\infty)$ is from (36).

4. Performance analysis

The performance of acquisition is generally measured with the mean acquisition time, which is the averaged time for correct acquisition. The mean acquisition time of the proposed system is a function of the probability of false alarm, the probability of missing (denoted as P_M), and the probability of correct acquisition (denoted as P_D). In this section, we will first derive these probabilities and then calculate the mean acquisition time.

4.1. Mean acquisition time

As mentioned, the proposed scheme performs sequential cell testing. Since there are Q possible cells, there are Q possible states in the system. Label these states as $\{s_0,\ldots,s_{Q-1}\}$ in the circular state diagram [1], as shown in Fig. 2. In the figure, the state labeled as ACQ indicates the state of correct acquisition. That labeled as FA is the state of false alarm. Using this diagram, we can evaluate the averaged time reaching the ACQ state, i.e., the mean acquisition time. Without loss of generality, we assume s_{Q-1} being the state of an inphase cell, and thus it is connected to the ACQ state. Also, let $Z^q \triangleq \|\mathbf{w}_{\mathrm{s,o}}^q(N)\|^2$. As described in Section 2, the optimum $\mathbf{w}_{\mathrm{s,o}}^q$, for outphase cells are all-zero vectors, and the corresponding Z^q should be small. On the other hand, Z^q of the inphase cell should be large. Using this property, we set a threshold ζ for the detection of the inphase cell. Thus, the acquisition problem can be seen as a hypothesis testing problem. Note that correct acquisition means that the inphase cell is correctly detected and at the same time the optimum peak-weight location (Δ) is also correctly estimated. There are two types of false alarm. We name the false alarm occurring in an inphase cell as an inphase false alarm, which means that the inphase cell is correctly detected but the peak location is not (i.e., $\hat{\Delta}\neq\Delta$), and the false alarm occurring in an outphase cell as an outphase false alarm.

From Fig. 2, we can see that the transfer function (TF) between s_{Q-1} and ACQ can be expressed as $H_b(\mathsf{z}) = P_{\mathrm{D}}\mathsf{z}^{N+1}$ [1,8,9], where $N+1$ denotes the time for iteration and cell detection, and z the unit-delay operator. The probability of missing, P_{M}, is defined as the probability of $Z^{Q-1}<\zeta$. Thus, if only the missing is considered, the TF between s_{Q-1} and s_0 can be expressed as $H_a(\mathsf{z}) = P_{\mathrm{M}}\mathsf{z}^{N+1}$. The probability of the inphase false alarm, denoted as P_{Fi}, is equal to $P_{\mathrm{Fi}} = 1 - P_{\mathrm{D}} - P_{\mathrm{M}}$. On the other hand, if only the inphase false alarm is considered, the TF between s_{Q-1} and FA can be expressed $H_f(\mathsf{z}) = P_{\mathrm{Fi}}\mathsf{z}^{N+1}$. Note the system has to stay T_{p} chips once it enters the FA state. The quantity T_{p} is generally referred to as the penalty time [1]. The TF between the input and the output of the FA state can be described as $H_d(\mathsf{z}) = \mathsf{z}^{T_{\mathrm{p}}}$. Thus, we can have the TF between s_{Q-1} and s_0 as $H_g(\mathsf{z}) \triangleq H_a(\mathsf{z}) + H_f(\mathsf{z})H_d(\mathsf{z})$. The TF between any s_q, $q=0,1,\ldots,Q-2$, and the FA state will be $H_c(\mathsf{z}) = P_{\mathrm{Fo}}\mathsf{z}^{N+1}$, where P_{Fo} is the probability of outphase false alarm.

If the outphase false alarm between two consecutive states, s_q and s_{q+1}, $q=0,1,\ldots,Q-2$, is not considered, then the TF between these two consecutive states can be described as $H_e(\mathsf{z}) = (1-P_{\mathrm{Fo}})\mathsf{z}^{N+1}$. Thus, we can have the TF between any two consecutive states, s_q and s_{q+1}, $q=0,1,\ldots,Q-2$, as $H_h(\mathsf{z}) \triangleq H_e(\mathsf{z}) + H_c(\mathsf{z})H_d(\mathsf{z})$.

Using the TFs derived above, we now can redraw the diagram in Fig. 2 as that in Fig. 3. In what follows, we use Fig. 3 to calculate the mean acquisition time. We define the probability of correct acquisition starting from time zero and ending at time n as $P_{\mathrm{ACQ}}(n)$. Then, its z-transform is given by

$$P_{\mathrm{ACQ}}(\mathsf{z}) = \sum_{n=0}^{\infty} P_{\mathrm{ACQ}}(n)\mathsf{z}^n, \tag{43}$$

which can be the generating function of acquisition time. Denote the mean acquisition time as T_{acq} and it can be derived from [1]

$$T_{\mathrm{acq}} \triangleq \frac{\mathrm{d}}{\mathrm{d}\mathsf{z}} P_{\mathrm{ACQ}}(\mathsf{z})|_{\mathsf{z}=1}. \tag{44}$$

Note that the unit of (44) is chip. Assuming that we can start searching at any state in $\{s_0,\ldots,s_{Q-1}\}$ with

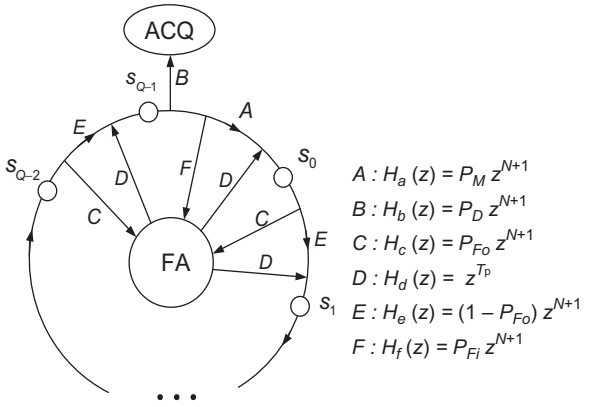

Fig. 2. Circular state diagram of the proposed system.

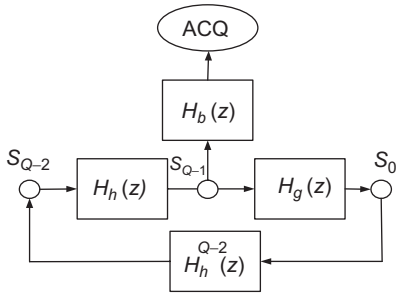

Fig. 3. Simplified state diagram.

equal probability $1/Q$, we rewrite (43) as

$$P_{\mathrm{ACQ}}(\mathsf{z}) = \frac{1}{Q}\sum_{q=0}^{Q-1} P_{q,\mathrm{ACQ}}(\mathsf{z}) \tag{45}$$

$$= \frac{1}{Q} H_b(\mathsf{z}) \sum_{q=0}^{Q-1} P_{q,Q-1}(\mathsf{z}), \tag{46}$$

where $P_{q,\mathrm{ACQ}}(\mathsf{z})$ denotes the TF between s_q and ACQ states, and $P_{q,Q-1}(\mathsf{z})$ the TF between s_q and s_{Q-1}. Using Fig. 3, we can have

$$P_{q,Q-1}(\mathsf{z}) = \frac{H_h^{Q-1-q}(\mathsf{z})}{1 - H_g(\mathsf{z}) H_h^{Q-1}(\mathsf{z})}. \tag{47}$$

Substituting (47) into (46), we obtain

$$P_{\mathrm{ACQ}}(\mathsf{z}) = \frac{1}{Q} \frac{H_b(\mathsf{z})}{1 - H_g(\mathsf{z}) H_h^{Q-1}(\mathsf{z})} \sum_{q=0}^{Q-1} H_h^{Q-1-q}(\mathsf{z}) \tag{48}$$

$$= \frac{1}{Q} \frac{H_b(\mathsf{z})[1 - H_h^{Q}(\mathsf{z})]}{[1 - H_g(\mathsf{z}) H_h^{Q-1}(\mathsf{z})][1 - H_h(\mathsf{z})]}. \tag{49}$$

Using (49) in (44), we finally obtain

$$T_{\mathrm{acq}} = \frac{1}{P_{\mathrm{D}}} \left\{ \left[1 + (Q-1)\frac{2 - P_{\mathrm{D}}}{2} \right](N+1) + \left[P_{\mathrm{Fi}} + (Q-1) P_{\mathrm{Fo}} \frac{2 - P_{\mathrm{D}}}{2} \right] T_{\mathrm{p}} \right\}. \tag{50}$$

Observing (50), we find that a large P_{Fo} and a small P_{D} can enlarge T_{acq} significantly. It should be noted that P_{Fo} is more harmful to T_{acq} than P_{Fi}. This is because there are $Q-1$ outphase cells and only one inphase cell. For an ideal situation that $P_{\mathrm{D}} = 1$ and $P_{\mathrm{Fi}} = P_{\mathrm{Fo}} = 0$, we have

$$T_{\mathrm{acq,LB}} = \frac{Q+1}{2}(N+1), \tag{51}$$

which can serve as the lower bound of (50).

4.2. Probabilities derivation

Since Z^q is random, we have to characterize its statistical properties. It is mentioned in [18] that when an adaptive filter approaches the steady state, its weights have a Gaussian distribution. From the analysis in the previous section, we see that in the steady state ($N \to \infty$), $\mathbf{w}_{\mathrm{s}}^q(N)$ has a mean vector of $\mathbf{w}_{\mathrm{s,o}}^q$ and $\mathbf{w}_{\mathrm{t}}^q(N)$ has a mean vector $\mathbf{w}_{\mathrm{t,o}}^q$. We denote their covariance matrices as $\mathbf{C}_{\mathrm{s}}^q \triangleq E\{[\mathbf{w}_{\mathrm{s}}^q(N) - \mathbf{w}_{\mathrm{s,o}}^q][\mathbf{w}_{\mathrm{s}}^q(N) - \mathbf{w}_{\mathrm{s,o}}^q]^{\mathrm{H}}\}$ and $\mathbf{C}_{\mathrm{t}}^q \triangleq E\{[\mathbf{w}_{\mathrm{t}}^q(N) - \mathbf{w}_{\mathrm{t,o}}^q][\mathbf{w}_{\mathrm{t}}^q(N) - \mathbf{w}_{\mathrm{t,o}}^q]^{\mathrm{H}}\}$, respectively. As a common practice, the step size is usually small. Thus, we can use the Taylor expansion to expand $1/(2 - \mu\lambda_{v,j}^q)$ in (35) with respect to $\mu\lambda_{v,j}^q = 0$. Then, we can derive

$$\frac{1}{2 - \mu\lambda_{v,j}^q} = \frac{1}{2} + \frac{1}{4}\mu\lambda_{v,j}^q + \cdots. \tag{52}$$

From (33), it can be seen that the matrix $\bar{\mathbf{P}}^q(n)$ will become diagonal as $n \to \infty$. Using this property and truncating the terms higher than the first-order in (52), we then have

$$\bar{\mathbf{P}}^q(n) = \frac{\mu}{2} J_{\min}^q \mathbf{I} + \frac{\mu^2}{4} J_{\min}^q \mathbf{\Lambda}^q. \tag{53}$$

Pre-multiplying and post-multiplying both sides of (53) with $\mathbf{U}^q$ and $[\mathbf{U}^q]^{\mathrm{H}}$, we obtain

$$\mathbf{P}^q(n) = \frac{\mu}{2} J_{\min}^q \mathbf{I} + \frac{\mu^2}{4} J_{\min}^q \mathbf{R}_v^q. \tag{54}$$

Note that the $M_{\mathrm{t}} \times M_{\mathrm{t}}$ upper-left submatrix of $\mathbf{P}^q(n)$ corresponds to $\mathbf{C}_{\mathrm{t}}^q$ and the $M \times M$ lower-right submatrix of that can be $\mathbf{C}_{\mathrm{s}}^q$. Thus, we can write

$$\mathbf{C}_{\mathrm{s}}^q = J_{\min}^q \left[\frac{\mu}{2}\mathbf{I} + \frac{\mu^2}{4}\mathbf{R}_r \right] \approx \frac{\mu J_{\min}^q}{2}\mathbf{I}, \tag{55}$$

$$\mathbf{C}_{\mathrm{t}}^q = J_{\min}^q \left[\frac{\mu}{2} + \frac{\mu^2}{4} \right] \mathbf{I} \approx \frac{\mu J_{\min}^q}{2}\mathbf{I}, \tag{56}$$

where $J_{\min}^q$ is the MMSE evaluated in Section 2. For notational clarity, we let $\sigma_1^2 \triangleq \mu J_{\min}^v/2$ and $\sigma_0^2 \triangleq \mu J_{\min}^q/2$, $q \neq v$. From (55)–(56), we can see that these filter weights are approximately independent and identically distributed (i.i.d.).

Let us calculate P_{D} now. Since $\mathbf{w}_{\mathrm{s,o}}^q = \mathbf{0}$ for $q \neq v$, we find that Z^q, $q \neq v$ is chi-square distributed with M degrees of freedom, while Z^v is noncentral chi-square distributed with M degrees of freedom. Thus, the probability of P_{Fo} is given by

$$P_{\mathrm{Fo}} = \int_{\zeta}^{\infty} \frac{1}{\sigma_0^M 2^{M/2} \Gamma(M/2)} \beta^{M/2-1} \exp\left(-\frac{\beta}{2\sigma_0^2} \right) \mathrm{d}\beta, \tag{57}$$

where $\Gamma(\cdot)$ stands for the gamma function [19], and ζ is usually selected on some level to prevent a large P_{Fo} (e.g. $P_{\mathrm{Fo}} = 0.01$). Let P_{C} be the probability of correct inphase cell detection. Then,

$$P_{\mathrm{C}} \triangleq \int_{\zeta}^{\infty} \frac{1}{2\sigma_1^2} \left(\frac{\beta}{s^2} \right)^{(M-2)/4} \exp\left(-\frac{s^2 + \beta}{2\sigma_1^2} \right) I_{M/2-1} \times \left(\sqrt{\beta}\frac{s}{\sigma_1^2} \right) \mathrm{d}\beta, \tag{58}$$

where $s^2 \triangleq \|\mathbf{w}_{\mathrm{s,o}}^v\|^2$ and $I_{M/2-1}(\cdot)$ the $(M/2-1)$th order modified Bessel function of the first kind [19]. Next, we evaluate the probability of $\hat{\Delta}=\Delta$, say P_Δ. Let $Y_j = |w_{\mathrm{t},j}^v(N)|^2$ for $j=0,\ldots,M_\mathrm{t}-1$. When N is large enough, Y_Δ has a noncentral chi-square distribution with two degrees of freedom, whereas Y_j, $j\neq\Delta$, has a chi-square distribution. The corresponding probability density functions can be shown as

$$p_{Y_\Delta}(y) = \frac{1}{2\sigma_\mathrm{i}^2}\exp\left(-\frac{|w_{\mathrm{t,o},\Delta}^v|^2+y}{2\sigma_\mathrm{i}^2}\right) I_0\left(\sqrt{y}\frac{|w_{\mathrm{t,o},\Delta}^v|}{\sigma_\mathrm{i}^2}\right), \tag{59}$$

$$p_{Y_j}(y) = \frac{1}{2\sigma_\mathrm{i}^2}\exp\left(-\frac{y}{2\sigma_\mathrm{i}^2}\right), \quad y>0, \quad j\neq\Delta, \tag{60}$$

where $w_{\mathrm{t,o},\Delta}^v$ denotes the $(\Delta+1)$th element in $\mathbf{w}_{\mathrm{t,o}}^v$ with $|w_{\mathrm{t,o},\Delta}^v|^2=1$. With (59)–(60), P_Δ is given by

$$P_\Delta = \Pr(Y_j < Y_\Delta) \tag{61}$$

$$= \int_0^\infty \left[\int_0^\beta p_{Y_j}(\beta')\,\mathrm{d}\beta'\right]^{M_\mathrm{t}-1} p_{Y_\Delta}(\beta)\,\mathrm{d}\beta, \quad j\neq\Delta, \tag{62}$$

where the i.i.d. property has been applied in (62). Finally, we can have $P_\mathrm{D}=P_\mathrm{C}P_\Delta$, $P_\mathrm{M}=1-P_\mathrm{C}$, $P_\mathrm{Fi}=1-P_\mathrm{D}-P_\mathrm{M}$. Then, (50) can be evaluated.

5. Simulation results

To demonstrate the effectiveness of the proposed system, we report some simulation results in this section. First, we set common parameters used in simulations as follows: $U=256$, $M=8$, $K=8$, $T_\mathrm{p}=100U$ chips, $\sigma_\eta^2=1$, $\mu=3\times10^{-3}$, $\mathbf{w}_\mathrm{s}^q(0)=\mathbf{0}$, and $\mathbf{w}_\mathrm{t}^q(0)=(1/\sqrt{M_\mathrm{t}})[1,\ldots,1]^\mathrm{T}$ for $q=0,\ldots,Q-1$. Also, for convenience, the DoAs are fixed to be $\{\phi_k\}_{k=1}^K=\{0.41,0.56,0.78,-0.20,-0.52,-1.12,1.12,0.94\}$ (radians) in all simulations.

In the first set of simulations, we examine the convergence behaviors of the proposed adaptive system. This includes the MSE convergence of the system, the SINR convergence behavior of the spatial filter, and the weight convergence of the temporal filter. All experimental results are derived from an average of 400 trials. In these experiments, we let $M_\mathrm{t}=8$, the array input SINR be -10 dB ($\alpha=1$), and the powers of jammers be equal. Fig. 4 shows the MSE convergence curve for the proposed system with the inphase cell ($q=v$). It can be seen that the steady-state MSE value approaches to the theoretical value 0.28 around $n=1300$. The theoretical MSE value is calculated from (37). In the same figure, we also show the MSE with an outphase cell ($q\neq v$). It is apparent that the experimental MSE is more fluctuating. This is because that $J_{\min}^q$, $q\neq v$, is much greater than $J_{\min}^v$ making the corresponding excess MSE larger. Fig. 5 illustrates the SINR convergence curve for the beamformer output [see $\gamma(n)$ in (38)]. The SINR starts from -11 dB and eventually reaches the optimum value 4.18 dB. The theoretical value is derived from (42) and is shown with the horizontal line in the figure. We omit the results for $q\neq v$, in which the experimental SINR is around -10 dB. This indicates that the spatial filter cannot suppress interference for outphase cells. From the figure, we conclude that the adaptive

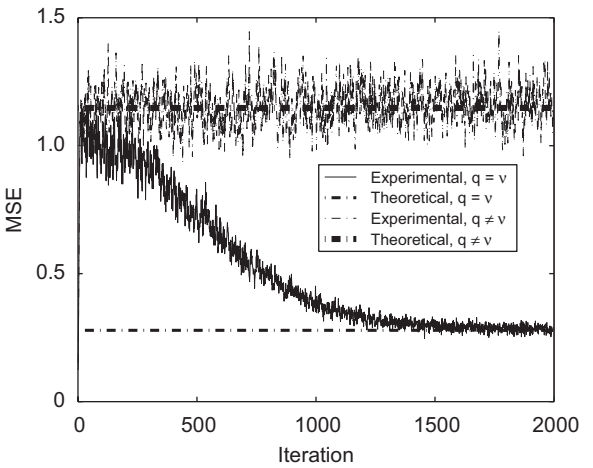

Fig. 4. Convergence curve for MSE when $\mu=3\times10^{-3}$ and $M_\mathrm{t}=8$. Theoretical value is from (37).

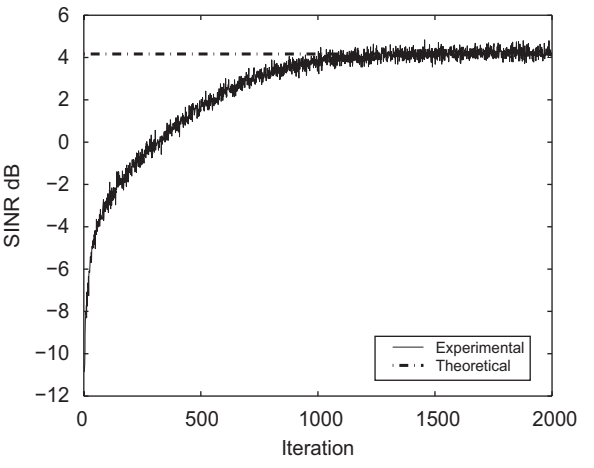

Fig. 5. Convergence curve for SINR of $\gamma(n)$ at an inphase cell, $\mu=3\times10^{-3}$ and $M_\mathrm{t}=8$. Theoretical value is from (42).

spatial filter can effectively suppress interference when it operates in the inphase cell. Fig. 6 presents several experimental beam patterns calculated from $\mathbf{w}_s^v(N)$. Here, we let $N = 2000$. The optimum beam pattern, derived from (17), is also shown. Note that the arrow signs indicate the signal DoAs and only the DoA of the desired user, ϕ_1, is labeled. As seen, the spatial filter, acting as a beamformer, can steer the main beam to the incident direction ϕ_1 and put nullities in the directions of interference. The convergence behavior of the temporal filter weights is shown in Fig. 7. We can see that the tap weight whose indices correspond to the code delay, $|w_{t,\Delta}^v(n)|^2$, converges to unity, while other weights, $|w_{t,j}^v(n)|^2$, $j \neq \Delta$, converge to a very small value (only one weight is shown in the figure).

In Figs. 8 and 9, we can see that the theoretical results calculated using derived formulas all match the simulated ones very well. Then, we calculate the mean acquisition time of the proposed system. Before that, we have to evaluate related probabilities. Fig. 8 shows the comparison of experimental and theoretical P_{Fo} (versus ζ). Here, the array input SINR is set as -10 dB. As we can see, P_{Fo} decreases rapidly as the threshold increases. The experimental results with $M_t = 8$ match the theoretical results [in (57)] better than those with $M_t = 16$. We also see that the experimental results for $N = 1000$ and $N = 2000$ are close. Fig. 9 shows the similar comparison for P_C. Here, experiment and theoretical results agree very well for $N = 2000$. However, they agree poorly for $N = 1000$. This is because the spatial

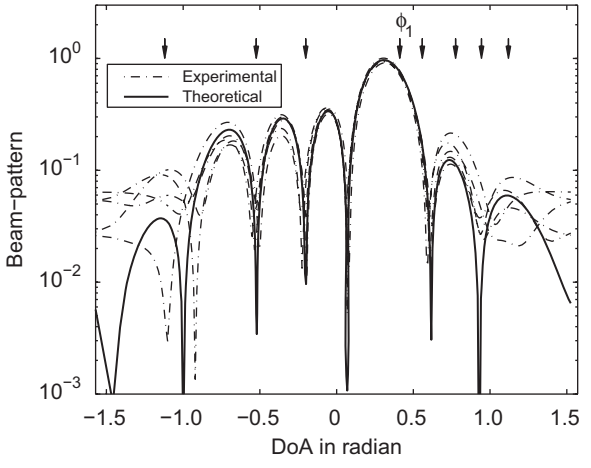

Fig. 6. Experimental and theoretical beam patterns for an inphase cell ($N = 2000$, $M_t = 8$, and $M = 8$). Arrow signs indicate the DoAs associated with all users. The labeled one, ϕ_1, is the DoA of the desired user.

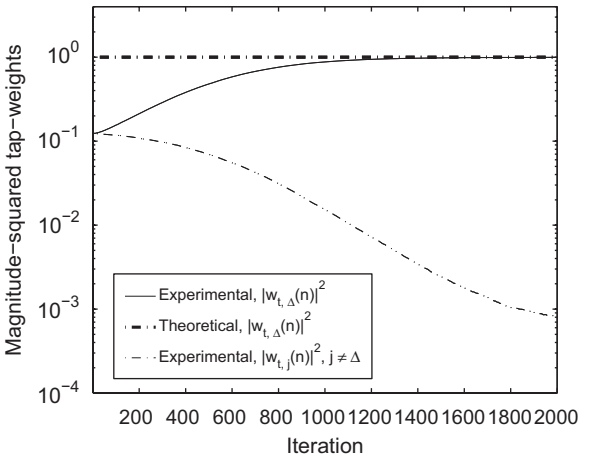

Fig. 7. Convergence curve for squared temporal filter weights $|w_{t,j}^v(n)|^2$ for $j = 0, \ldots, M_t - 1$ and $M_t = 8$. Theoretical value is obtained from (16).

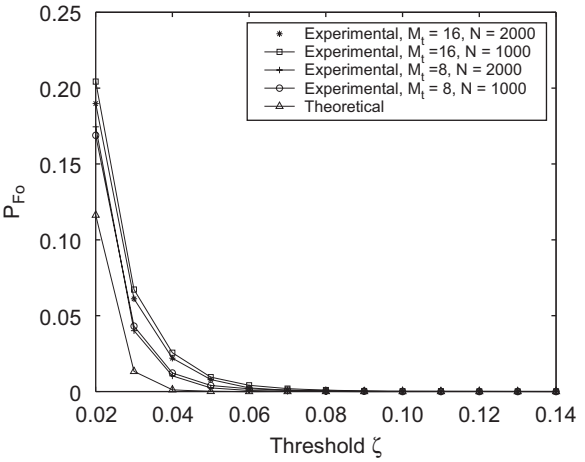

Fig. 8. Experimental and theoretical probabilities of outphase false alarm P_{Fo} versus threshold ζ.

filter has not converged with the given number of iterations, and Z^v tends to be smaller than the threshold. This behavior is different from that in P_{Fo} calculation. From Figs. 8 and 9, we can see that the best ζ is around 0.07. Using this value, P_{Fo} can be close to 0 and P_C to 1. The theoretical value of P_Δ is usually very close to 1. With 10^4 trials, we find $P_\Delta = 1$ ($N = 2000$, $M_t = 8$ or $M_t = 16$). As a result, we can let $P_C \approx P_D$. Since the interference is mainly suppressed by the spatial filter, P_{Fi} is close to 0. Substituting derived experimental probabilities into (50), we can then calculate the mean acquisition time. Fig. 10 shows the result. In the figure, lower bounds derived from (51), are also shown. It is simple to see that if ζ is too small, P_{Fo} will be large,

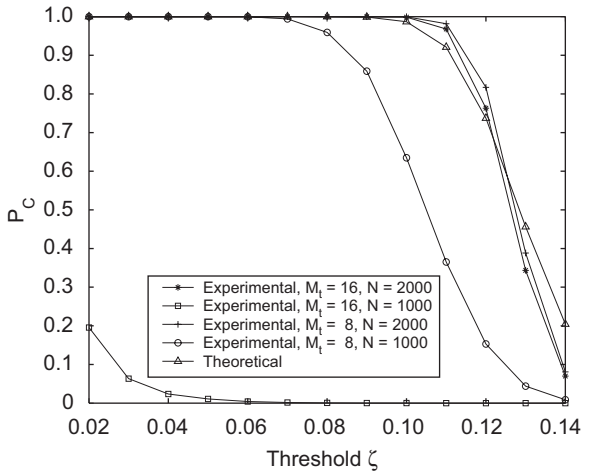

Fig. 9. Experimental and theoretical probabilities of P_C versus threshold ζ.

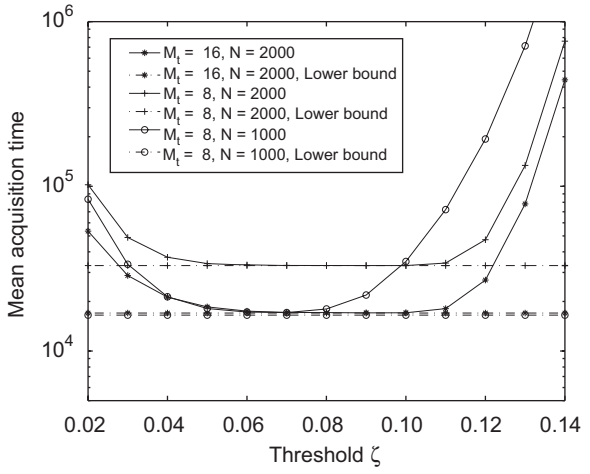

Fig. 10. Experimental mean acquisition time (chips) versus ζ.

leading to large mean acquisition time. On the contrary, if ζ is too large, P_M being equal to $1-P_C$ will be large, leading to large mean acquisition time also. From the figure, we can observe that ζ can be chosen in a wide range of value such that mean acquisition times can approach lower bounds.

Finally, we conduct performance comparison for the correlator-based scheme in [13], the adaptive array system in [16], and the proposed system. We let $U=256$, $\sigma_\eta^2=1$, $\alpha=1$, and the powers of all jammers be equal. As addressed in [13], the derived theoretical threshold is not accurate enough to guarantee that a designated probability of false alarm (set as 0.01 here) can be achieved. Thus, we experimentally search for the threshold, processing

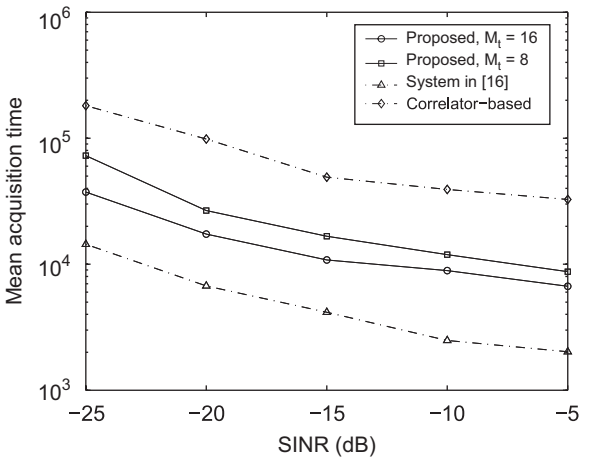

Fig. 11. Mean acquisition time comparison for $U=256$.

period (for adaptation), and step size that gives the minimal mean acquisition time (for each array input SINR). To ensure a fair comparison, we also search for an optimum set $\{\mu, N, \zeta\}$ that provides the optimum performance for the proposed system ($M_t=8$ or 16). Here, P_{Fo} is set as 0.01. Similarly, for the system in [16], the performance is optimized over $\{\mu, N\}$. Fig. 11 shows the performance comparison for these systems in various SINRs. From the figure, we first can see that the correlator-based system has the worst performance. This is because the beamformer training cannot be accomplished in a short processing period, especially in serious MAI environments. The system in [16] exhibits the best performance. It can outperform the correlator-based system by an order of magnitude. Comparing to that in [16], the proposed system somewhat compromises the performance. However, its computational complexity is much lower. For example, with $M_t=8$, the temporal filter size is just $\frac{1}{32}$ of that in [16]. We also can see that for the proposed system with $M_t=8$ performs slightly worse than that with $M_t=16$. We can expect that the larger the M_t, the smaller the performance loss. Thus, we can have an easy tradeoff between performance and computational complexity.

6. Conclusions

In this paper, we proposed a low-complexity adaptive array code acquisition scheme, especially being suited to large-delay channel environments. Applying the serial-search technique, we can greatly reduce the temporal filter size, so does the

computational complexity. The proposed scheme also allows an easy tradeoff between performance and computational complexity. With the special designed structure, the proposed system is able to suppress MAI and estimate code delay simultaneously. It can outperform the conventional correlator-based system. We also analyze the convergence behavior and the mean acquisition time of the proposed scheme, and derive related closed-form expressions. Simulations verify that theoretical and experimental results agree well. In this paper, we only consider the flat-fading yet integer chip-delay channels. With minor modifications, the proposed system can be easily extended to multi-path yet fractional chip-delay channels [16]. This issue may serve as a topic for further research.

References

[1] A. Polydoros, C. Weber, A unified approach to serial search spread-spectrum code acquisition—part I and II, IEEE Trans. Commun. 32 (May 1984) 542–560.
[2] A.J. Viterbi, Principle of Spread Spectrum Communications, Addison-Wesley, New York, 1995.
[3] U. Madhow, M.B. Pursley, Acquisition in direct-sequence spread-spectrum communication networks: an asymptotic analysis, IEEE Trans. Inform. Theory 39 (3) (May 1993) 903–912.
[4] T.K. Moon, R.T. Short, C.K. Rushforth, Average acquisition time for SSMA channels, in: IEEE Military Communication Conference, 1991, pp. 1042–1046.
[5] D. Zheng, J. Li, S.L. Miller, E.G. Ström, An efficient code-timing estimator for DS-CDMA signals, IEEE Trans. Signal Process. 45 (January 1997) 82–89.
[6] E.G. Ström, et al., Propagation delay estimation in asynchronous direct-sequence code-sequence multiple access systems, IEEE Trans. Commun. 44 (January 1996) 84–93.
[7] M.G. El-Tarhuni, A.U. Sheikh, An adaptive filtering PN code acquisition scheme with improved acquisition based capacity in DS/CDMA, in: 9th IEEE International Symposium on Personal, Indoor, and Mobile Radio Communications, vol. 3, 1998, pp. 1486–1490.
[8] M.G. El-Tarhuni, A.U. Sheikh, Adaptive synchronization for spread spectrum systems, in: IEEE Vehicular Technology Conference, vol. 1, April 1996, pp. 170–174.
[9] M.G. El-Tarhuni, Application of adaptive filtering to direct-sequence spread-spectrum code synchronization, Ph.D. Dissertation, Department of System and Computer Engineering, Carleton University, Canada, 1997.
[10] R.F. Smith, S.L. Miller, Acquisition performance of an adaptive receiver for DS-CDMA, IEEE Trans. Commun. 47 (9) (September 1999).
[11] H.L. Yang, W.R. Wu, Multirate adaptive filtering for DS/CDMA code acquisition, in: IEEE International Symposium on Signal Processing and Information Technology, December 2003, pp. 363–366.
[12] Y. Zhang, L. Zhang, G. Liao, PN code acquisition and beamforming weight acquisition for DS-CDMA systems with adaptive array, in: 14th IEEE International Symposium on Personal, Indoor, and Mobile Radio Communications, vol. 2, 2003, pp. 1385–1389.
[13] B. Wang, H.M. Kwon, PN code acquisition using smart antenna for spread-spectrum wireless communications—part I, IEEE Trans. Veh. Technol. 52 (1) (January 2003) 142–149.
[14] S. Kim, Approximate maximum likelihood approach for code acquisition in DS-CDMA systems with multiple antennas, IEICE Trans. Commun. E 88-B (3) (March 2005) 1054–1065.
[15] H.L. Yang, W.R. Wu, A novel adaptive code acquisition using antenna array for DS/CDMA systems, in: IEEE International Workshop on Antenna Technology: Small Antennas and Novel Metamaterials, March 2005.
[16] H.L. Yang, W.R. Wu, A novel adaptive antenna array for DS/CDMA code acquisition, IEEE Trans. Signal Process. 55 (9) (2007) 4567–4580.
[17] S. Haykin, Adaptive Filter Theory, 3rd ed., Prentice-Hall, New Jersey, 1996.
[18] N.J. Bershad, L.Z. Qu, On the probability density function of the LMS adaptive filter weights, IEEE Trans. Acoust. Speech Signal Process. 37 (1) (January 1989) 43–56.
[19] J.G. Proakis, Digital Communications, 4th ed., McGraw-Hill, New York, 2000.